EurJOC
European Journal of Organic Chemistry

FULL PAPER

DOI: 10.1002/ejoc.201300347

Subtle Steric Effects in Nickel-Catalysed Kumada–Tamao–Corriu Cross-Coupling Using Resorcinarenyl-Imidazolium Salts

Neslihan Şahin,[a,b] David Sémeril,*[a] Eric Brenner,[a] Dominique Matt,*[a] İsmail Özdemir,[c] Cemal Kaya,[c] and Loïc Toupet[d]

Keywords: Cavitands / Cross-coupling reactions / Ligand design / Carbene ligands / Nickel

Three resorcinarene-cavitands bearing a 3-R-1-imidazolylium substituent (R = alkyl) grafted to the wider rim of the cavitand (**1–3**) were assessed in the Kumada–Tamao–Corriu cross-coupling of aryl halides with arylmagnesium halides. Their combination with $[Ni(cod)_2]$ (cod = 1,5-cyclooctadiene; 1:1 stoichiometry) resulted in highly efficient catalysts, the activities of which varied in the following order: R = *n*-propyl (**1**) < isopropyl (**2**) ≈ benzyl (**3**). A remarkable turnover frequency of 60400 mol(ArX) mol(Ni)$^{-1}$ h^{-1} was obtained in the coupling of 2-bromo-6-methoxynaphthalene with PhMgBr (100 °C in dioxane, with precursor **2**). The high activities of the cavitand derivatives were attributed to steric effects that facilitate the reductive-elimination/product decoordination step. Comparative experiments carried out with a structurally modified resorcinarene, as well as cavity-free imidazolium salts bearing 2-methoxyaryl substituents, suggest that the efficiency of the catalysts mainly relies on steric interactions between the metal and the flexible substituents attached to two methine carbon atoms. These steric interactions are probably reinforced each time the metal binds one of the two oxygen atoms located next to the catalytic centre.

Introduction

Known since 1972,[1–4] the Kumada–Tamao–Corriu (KTC) reaction, i.e., the cross-coupling of a Grignard reagent (ArMgX) with an aryl halide, belongs to a family of valuable methods commonly used for carbon–carbon bond formation.[5–7] Although such reactions are most often performed with palladium,[8] they can also be carried out with more cost-efficient nickel catalysts. Preferred KTC Ni-catalysts are based on diphosphanes capable of forming large chelate rings, for example, $Ph_2P(CH_2)_3PPh_2$, $Ph_2P(CH_2)_4PPh_2$, $[Fe(C_5H_4PPh_2)_2]$[9,10] or some calix[4]arenyl-diphosphanes,[11,12] although monodentate ligands (e.g., PCy_3,[13] calixarenyl-phosphanes,[14] iminophosphoranes,[15] diaminophosphane oxides,[16] alkyl-imidazoles[17] and carbenes[18–27]) have also been employed successfully.

We have recently started a programme aimed at the use of resorcin[4]arene-derived cavitands as platforms for the preparation of expanded ligands.[28–31] Among these, the imidazolium salts **1**–**3**, which are precursors of N-heterocyclic carbene (NHC) ligands, efficiently promote palladium-catalysed cross-coupling between arylboronic acids and aryl halides.[32] This remarkable efficiency was attributed to a combination of steric bulk provided by the resorcinarenyl fragment and to the presence of oxygen atoms within the macrocyclic backbone that are able to temporarily coordinate the metal centre. With the aim of extending the scope of applications of these proligands, we have now investigated their performance in nickel-catalysed KTC coupling.

Results and Discussion

Imidazolium salts **1**–**3** were prepared from the readily available tetrabrominated cavitand **4**.[32] The reaction sequence for each synthesis (Scheme 1) began with an Ullmann[33] coupling (imidazole/**4** ratio 1:1), leading to a mixture (M1) of mono-imidazolyl resorcinarenes, which were chromatographically separated as a whole from another mixture of minor species (M2). As inferred from NMR spectra, some of the mono-imidazole derivatives of M1 did not contain the expected number of Br atoms. We therefore reacted this mixture with *n*BuLi and quenched the resulting solution with MeOH, which gave imidazolyl-resorcinarene **5** selectively (30% overall yield). Imidazolium salts **1**–**3** were then obtained quantitatively by alkylation of **5** with the appropriate alkyl bromide (Scheme 1).

---

[a] Université de Strasbourg, Laboratoire de Chimie Inorganique Moléculaire et Catalyse, UMR 7177 CNRS,
1 rue Blaise Pascal, 67008 Strasbourg Cedex, France
E-mail: dsemeril@unistra.fr
dmatt@unistra.fr
Homepage: http://inorganics.online.fr
[b] Department of Chemistry, Faculty of Science, Cumhuriyet University,
Sivas, 58140, Turkey
[c] Department of Chemistry, Faculty of Science and Art, Inönü University,
Malatya, 44280, Turkey
[d] Institut de Physique, UMR 6251 CNRS, Université de Rennes 1,
Campus de Beaulieu, 35042 Rennes Cedex, France

Supporting information for this article is available on the WWW under http://dx.doi.org/10.1002/ejoc.201300347.

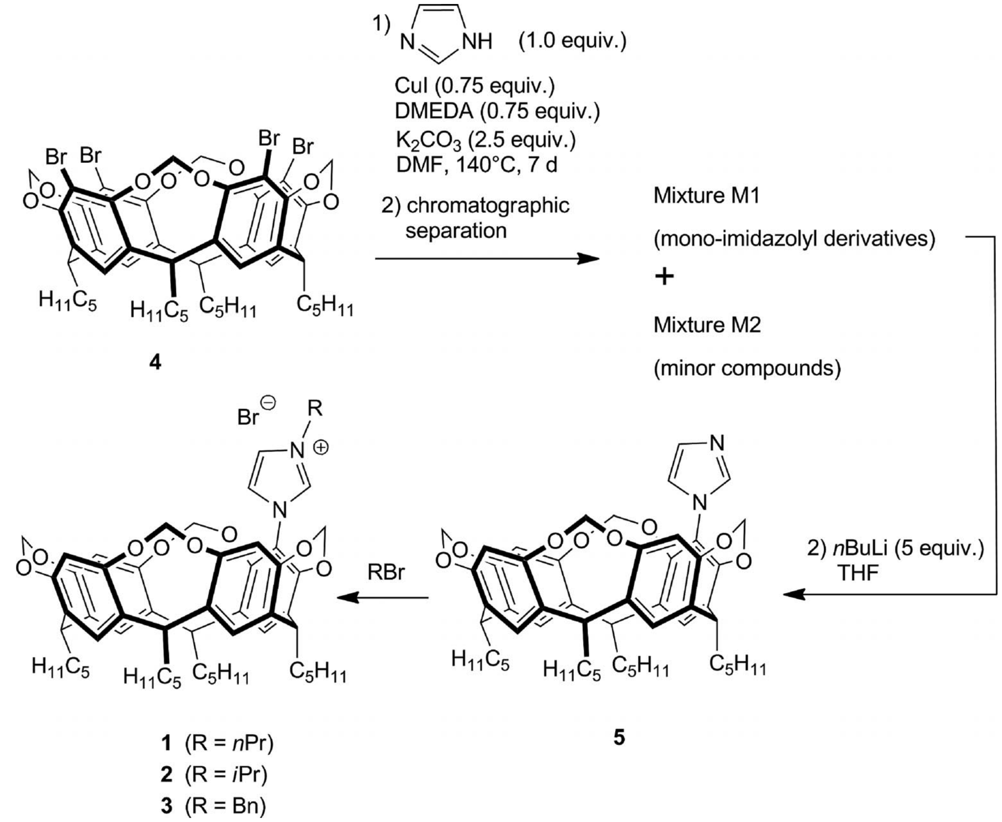

Scheme 1. Synthesis of imidazolium salts **1**–**3**.

The solid-state structures of imidazolium salts **1** and **2** were established by single-crystal X-ray diffraction (Figure 1). In each case the unit cell contains two molecules (**1a**/**1b** and **2a**/**2b**), which differ only slightly. The core of the macrocycles adopt the usual bowl-shaped structure found in hundreds of reported resorcinarene cavitands. The upper rim diameters (defined as the segments linking the OC*C*CO carbon atoms of opposite resorcinolic rings) are 7.97 and 8.00 Å (mean) for the two conformers of **1** and 7.98 and 7.98 Å (mean) for those of **2**. A molecule of diisopropyl ether is poised above the cavity of compound **1**. In both compounds, the procarbenic carbon atom is turned away from the cavity. The bromide anion, which lies approximately on the cavity axis, is located within the domain delineated by the four pentyl chains.

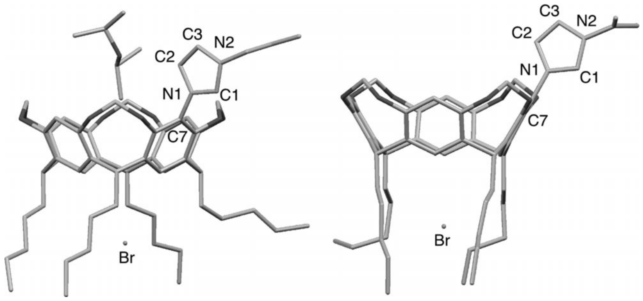

Figure 1. Structures of the molecules (ion pairs) found within the lattices of **1** (left) and **2** (right); only one of the two very similar molecules of each unit cell is shown. For clarity, external solvent molecules are not shown. Important distances [Å] and angles [°]: For **1**: N1–C1 1.343(6), N2–C1 1.320(6), N1–C7 1.430(5), C1–N1–C2 108.4(4), C1–N2–C3 109.6(4), N1–C1–N2 108.1(4); For **2**: N1–C1 1.361(10), N2–C1 1.340(11), N1–C7 1.437(10), C1–N1–C2 110.0(7), C1–N2–C3 109.0(8), N1–C1–N2 106.5(9).

Catalytic Kumada–Tamao–Corriu Cross-Coupling

Cross-coupling tests (Scheme 2) were conducted with a set of eight aryl halides (six bromides and two chlorides), and two aryl Grignard reagents, PhMgBr and *o*-TolMgCl. The catalytic systems, which were expected to involve NHC complexes, were all generated in situ by mixing the imidazolium salt with an appropriate nickel precursor.

Scheme 2. Kumada–Tamao–Corriu cross-coupling reaction.

Optimising the Catalytic Conditions

Runs to determine the best catalytic conditions were carried out using 4-bromoanisole, phenylmagnesium bromide and imidazolium salt **3**, with a nickel loading of 0.01 mol-%. The conversions were determined after one hour reaction time at 100 °C. We first investigated the influence of the nickel precursors. These tests were carried out with an imidazolium salt/nickel ratio of 1:1. Under these conditions, use of $[\mathrm{Ni(cod)_2}]$ led to a conversion (61.8%) that was significantly higher than that obtained with $[\mathrm{Ni(OAc)_2}]$ or $[\mathrm{NiBr_2(dme)}]$ (Table 1, entries 1–3). Applying imidazolium/Ni ratios higher than 1:1 resulted in a decrease in conversion, which reached a plateau of ca. 44% for a ratio of 2:1 (Table 1, entries 3–6). Reducing the PhMgBr/4-bromoanisole ratio from 2 to 1 reduced the catalyst activity, with the conversion dropping from 61.8 to 43.7% (Table 1, entries 3 and 8). As expected, working at lower temperatures resulted in a decrease in the reaction rate (Table 1, entries 3 and 9–11). Detailed GC analysis revealed the presence of some homocoupling product, however, its proportion never exceeded 13%.

Table 1. Kumada–Tamao–Corriu cross-coupling of 4-bromoanisole with phenylmagnesium bromide; the search for optimal catalytic conditions.[a]

Entry	Nickel precursor	Imidazolium/ nickel ratio	PhMgBr [mmol]	T [°C]	Conversion [%]
1	$[\mathrm{Ni(OAc)_2}]$	1:1	1.00	100	55.6
2	$[\mathrm{NiBr_2(dme)}]$	1:1	1.00	100	36.4
3	$[\mathrm{Ni(cod)_2}]$	1:1	1.00	100	61.8
4	$[\mathrm{Ni(cod)_2}]$	1.5:1	1.00	100	54.3
5	$[\mathrm{Ni(cod)_2}]$	2:1	1.00	100	43.4
6	$[\mathrm{Ni(cod)_2}]$	5:1	1.00	100	44.6
7	$[\mathrm{Ni(cod)_2}]$	1:1	0.75	100	46.8
8	$[\mathrm{Ni(cod)_2}]$	1:1	0.50	100	43.7
9	$[\mathrm{Ni(cod)_2}]$	1:1	1.00	80	38.1
10	$[\mathrm{Ni(cod)_2}]$	1:1	1.00	50	23.0
11	$[\mathrm{Ni(cod)_2}]$	1:1	1.00	25	14.1

[a] Rection conditions: [Ni] (5×10^{-5} mmol, 1×10^{-2} mol-%), imidazolium salt **3**, 4-bromoanisole (0.5 mmol), PhMgBr, dioxane (1.5 mL), decane (0.05 mL), 1 h. The conversions were determined by GC analysis, the calibrations being based on decane.

Table 2. Kumada–Tamao–Corriu cross-coupling of aryl bromides catalysed by $[\mathrm{Ni(cod)_2}]$/imidazolium salts.

Entry	ArBr		Imidazolium salt		
			1	**2**	**3**
1[a]	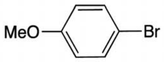	conv. (%)	49.4	55.9	61.8
		TOF	4940	5590	6180
2[a]	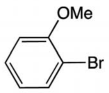	conv. (%)	35.4	32.4	32.1
		TOF	3540	3240	3210
3[a]	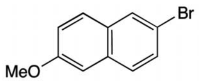	conv. (%)	85.5	89.3	87.5
		TOF	8550	8930	8750
4[b]		conv. (%)	51.7	60.4	55.9
		TOF	51700	60400	55900
5[a]	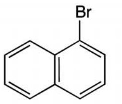	conv. (%)	91.8	92.0	88.1
		TOF	9180	9200	8810
6[b]		conv. (%)	24.3	28.3	27.8
		TOF	24300	28300	27800
7[a]	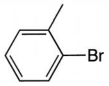	conv. (%)	35.8	52.6	55.3
		TOF	3580	5260	5530
8[a]	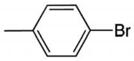	conv. (%)	55.3	53.9	66.3
		TOF	5530	5390	6630

[a] Reaction conditions: $[\mathrm{Ni(cod)_2}]$ (5×10^{-5} mmol, 1×10^{-2} mol-%), imidazolium salt (5×10^{-5} mmol, 1×10^{-2} mol-%), ArBr (0.5 mmol), PhMgBr (1 mmol), decane (0.05 mL), dioxane (1.5 mL), 100 °C, 1 h. The conversions were determined by GC analysis, the calibrations being based on decane. The TOFs are expressed in mol(ArBr) mol(Ni)$^{-1}$ h^{-1}. [b] Reaction conditions: $[\mathrm{Ni(cod)_2}]$ (5×10^{-6} mmol, 1×10^{-3} mol-%), imidazolium salt (5×10^{-6} mmol, 1×10^{-3} mol-%).

Catalytic Kumada–Tamao–Corriu Cross-Coupling of Arylbromides

As a general trend, under the optimal conditions determined above {imidazolium salt/$[\mathrm{Ni(cod)_2}]$ = 1:1 and ArMgX/ArBr = 2:1}, the reactivity increased with increasing bulk of the R substituent [*n*-propyl (**1**) < isopropyl (**2**) < benzyl (**3**)]. For example, 4-bromoanisole was converted into 4-methoxybiphenyl in 49.4, 55.9 and 61.8% yield, by using imidazolium salts **1**, **2** and **3**, respectively (Table 2, entry 1). Starting from 2-bromo-6-methoxynaphthalene or 1-bromonaphthalene, conversions of more than 85% were observed, irrespective of which imidazolium salt was employed (Table 2, entries 3 and 5). For the former substrate, and in the presence of **2**, reducing the catalyst loading to 0.001 mol-% led to a turnover frequency (TOF) of 60400 mol(ArBr) mol(Ni)$^{-1}$ h^{-1} (Table 2, entry 4).

As expected, near-complete conversions were achieved upon increasing the reaction time. For example, the sterically hindered 2-bromoanisole and 2-bromotoluene were converted in 87.8 and 87.4% yields, respectively, in 5 h using a catalyst loading of only 0.01 mol-% (Table 3, entries 3 and 7). Higher conversions were observed when 2-tolylmagnesium chloride was employed. With this Grignard reagent, the two *ortho*-substituted aryl bromides were fully converted within only 2 h (Table 3, entries 4 and 8).

Imidazolium salt **3** was further assessed in the cross-coupling of 2- and 4-chlorotoluene. Both chlorotoluenes were efficiently converted into biaryls in 1 h when the reactions

Table 3. Kumada–Tamao–Corriu cross-coupling of aryl bromides catalysed by [Ni(cod)$_2$]/imidazolium salt **3**.[a]

Entry	ArBr	ArMgX	Time (h)	Conversion (%)
1	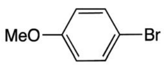	PhMgBr	3	85.6
2		*o*-TolMgCl	1	95.7
3	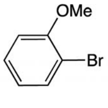	PhMgBr	5	87.8
4		*o*-TolMgCl	2	97.8
5	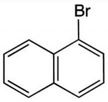	PhMgBr	3	100
6		*o*-TolMgCl	1	100
7	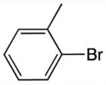	PhMgBr	5	87.4
8		*o*-TolMgCl	2	100
9	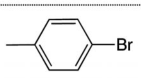	PhMgBr	3	82.2
10		*o*-TolMgCl	1	96.3

[a] Reaction conditions: [Ni(cod)$_2$] (5×10^{-5} mmol, 1×10^{-2} mol-%), imidazolium salt **3** (5×10^{-5} mmol, 1×10^{-2} mol-%), ArBr (0.5 mmol), RMgX (1 mmol), decane (0.05 mL), dioxane (1.5 mL), 100 °C, 1 h. The conversions were determined by GC analysis, the calibrations being based on decane.

Table 4. Kumada–Tamao–Corriu cross-coupling of 2- and 4-chlorotoluenes catalysed by [Ni(cod)$_2$]/imidazolium salt **3**.[a]

Entry	ArCl	[Ni(cod)$_2$] (mol %)	ArMgX	Temp. (°C)	Time (h)	Conv. (%)
1	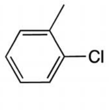	0.1	PhMgBr	100	5	45.6
2		1	PhMgBr	100	1	77.9
3		1	PhMgBr	50	24	98.2
4		1	PhMgBr	25	24	98.4
5		0.1	*o*-TolMgCl	100	5	64.7
6		1	*o*-TolMgCl	100	1	87.5
7		1	*o*-TolMgCl	50	24	100
8		1	*o*-TolMgCl	25	24	98.9
9	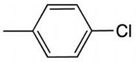	0.1	PhMgBr	100	24	88.5
10		1	PhMgBr	100	1	100
11		1	PhMgBr	50	24	100
12		1	PhMgBr	24	24	96.9
13		0.1	*o*-TolMgCl	100	24	74.8
14		1	*o*-TolMgCl	100	1	99.6
15		1	*o*-TolMgCl	50	24	98.5
16		1	*o*-TolMgCl	25	24	99.3

[a] Reaction conditions: [Ni(cod)$_2$], imidazolium salt **3** (1 equiv./Ni), ArCl (0.25 mmol), ArMgX (0.5 mmol), dioxane (0.75 mL), decane (0.025 mL). The conversions were determined by GC analysis, the calibrations being based on decane.

were performed in the presence of 1 mol-% nickel at 100 °C (Table 4, entries 2 and 10). In comparison, at a temperature of 25 °C, for example, the reaction with 2-chlorotoluene required 24 h to reach a conversion of 98% (Table 4, entry 4). Use of 2-tolylmagnesium chloride did not change the performance of the catalytic system (Table 4, entries 8 and 16).

To clarify the role of the resorcinarenyl fragment of proligands **1**–**3** during catalysis, we first investigated the properties of imidazolium salts devoid of a cavity, namely **6**–**8**, two of which have OMe substituents (Figure 2).[32] Under the optimised conditions described above, the conversions varied in the order **6** < **7** < **8**, increasing with number of methoxy (MeO) substituents (Table 5). MeO substituents may enhance the bulk of the NHC ligand formed and consequently facilitate reductive elimination and/or product decoordination. Furthermore, the MeO groups of **7** and **8**, like those of **1**–**3**, may bind the metal in a hemilabile fashion so as to make the metal not only sterically more crowded but also electron richer. The latter electronic contribution is however not relevant, as in nickel-catalysed KTC cross coupling, the first irreversible step is not oxidative addition, but π-coordination of the incoming ArX substrate.[34] The results presented in Table 5 clearly reveal that the performance of resorcinarene **3** surpasses that of its simple analogue **8** (Table 5), and thus cannot be dictated solely by the presence of potentially binding oxygen atoms. As already indicated, in KTC cross-coupling with nickel, the key step in the catalytic cycle is the substitution of the coordinated ArAr′ product by the incoming ArX substrate, a step that may be promoted by sterically demanding substituents. Molecular models show that [Ni(ArAr′)L] intermediates obtained from **3** have the catalytic centre either embedded in the cavity, thus creating a strong steric pressure of the cavity wall on the ArAr′ moiety, or be placed outside the cavity. In this latter case, steric interactions may arise between the metal centre and the pentyl groups, these being slightly reinforced if the metal binds an oxygen atom of the cavity (Figure 3). Note that formation of a C_{carbene},*O*-chelate complex is only possible with the metal located outside the cavity. To confirm or exclude a possible influence of the pentyl groups on the catalytic outcome, we prepared the imidazolium salt **9**, having remote, downwards-oriented phenyl groups instead of pentyl chains (rccc stereoisomer). The activity of the corresponding catalytic system turned out to be significantly weaker than that obtained from **3**, and close

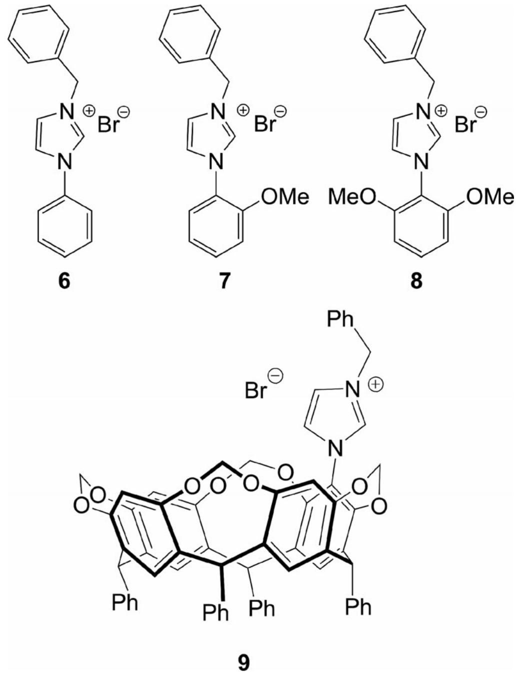

Figure 2. Imidazolium salts **6**–**9** used for ranking the resorcinarene derivatives **1**–**3** in KTC.

Table 5. Comparison of imidazolium salts in Kumada–Tamao–Corriu cross-coupling of aryl bromides.[a]

Entry	ArBr		Imidazolium salt				
			3	6	7	8	9
1	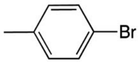	Conv. (%)	66.3	31.4	40.5	42.6	48.7
2	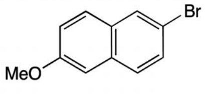	Conv. (%)	87.5	11.7	41.2	49.4	52.6
3	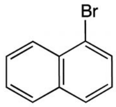	Conv. (%)	88.1	42.9	45.6	58.3	61.8

[a] Reaction conditions: [Ni(cod)$_2$] (5×10^{-5} mmol, 1×10^{-2} mol-%), imidazolium salt (5×10^{-5} mmol, 1×10^{-2} mol-%), ArBr (0.5 mmol), PhMgBr (1 mmol), decane (0.05 mL), dioxane (1.5 mL), 100 °C, 1 h. The conversions were determined by GC analysis, the calibrations being based on decane.

to that of the methoxy-substituted salt **8**. This observation demonstrates the beneficial role of the pentyl groups of **3** and also indicates that, during catalysis, intermediates with *exo*-oriented metal centres predominate.

Conclusions

We have demonstrated that the resorcinarenyl-imidazolium salts **1**–**3** constitute efficient ligand precursors for nickel-catalysed Kumada–Tamao–Corriu cross-coupling of aryl halides with arylmagnesium halides [Highest TOF observed in this study: 60400 mol(ArX) mol(Ni)$^{-1}$ h^{-1}]. Comparative studies with the phenyl-substituted resorcinarene **9**, as well as cavity-free imidazolium salts bearing 2-methoxyaryl substituents, imply that the efficiency of the catalysts mainly depend on steric interactions between the flexible pentyl groups and the metal centre; these result from an *exo* positioning of the nickel atom, and probably increase each time the metal binds one of the two neighbouring oxygen atoms. Further investigations are aimed at modifying the methine carbon atoms of the resorcinarene with appropriate substituents, so as to increase their steric interactions with the metal.

Experimental Section

General Methods: All syntheses were performed in Schlenk-type flasks under dry nitrogen. Solvents were dried by conventional methods and were distilled immediately prior to use. Routine ^{1}H and ^{13}C{^{1}H} NMR spectra were recorded with a Bruker AVANCE 300 or AVANCE 400 spectrometer. ^{1}H NMR spectra were referenced to residual protonated solvents (δ = 7.26 ppm for CDCl$_3$) and ^{13}C chemical shifts are reported relative to deuterated solvents (δ = 77.16 ppm for CDCl$_3$). Elemental analyses were performed by the Service de Microanalyse, Institut de Chimie, Université de Strasbourg.

5-*N*-(3-Propyl-1-imidazolylium)-4(24),6(10),12(16),18(22)-tetramethylenedioxy-2,8,14,20-tetrapentyl-resorcin[4]arene bromide (**1**),[32] 5-*N*-(3-isopropyl-1-imidazolylium)-4(24),6(10),12(16),18(22)-tetramethylenedioxy-2,8,14,20-tetrapentyl-resorcin[4]arene bromide (**2**),[32] 5-*N*-(3-benzyl-1-imidazolylium)-4(24),6(10),12(16),18(22)-tetramethylenedioxy-2,8,14,20-tetrapentyl-resorcin[4]arene bromide (**3**),[32] 5,11,17,23-tetrabromo-4(24),6(10),12(16),18(22)-tetramethylenedioxy-2,8,14,20-tetrapentyl-resorcin[4]arene (**4**),[28] 1-benzyl-3-phenyl-imidazolium bromide (**6**), 1-benzyl-3-(2-meth-

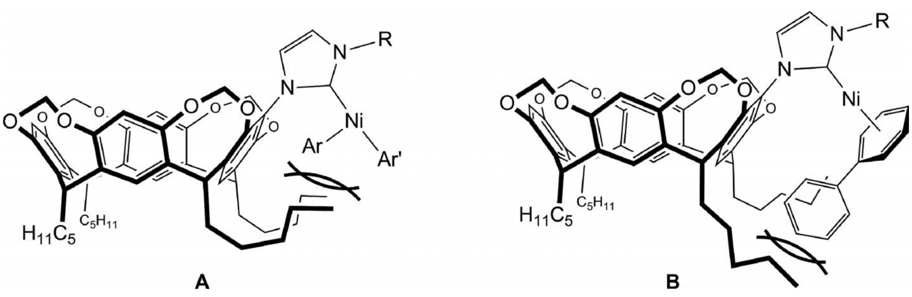

Figure 3. Steric interactions involving two pentyl substituents in possible *exo*-intermediates formed from resorcinarenes **1**–**3** during catalysis; the formation of the zerovalent complex B follows that of the Ni^{II} complex A.

oxyphenyl)imidazolium bromide (**7**),[32] 1-benzyl-3-(2,6-dimethoxyphenyl)imidazolium bromide (**8**),[32] 5-*N*-(3-benzyl-1-imidazolylium)-4(24),6(10),12(16),18(22)-tetramethylenedioxy-2,8,14,20-tetra-phenyl-resorcin[4]arene bromide (**9**)[32] and [Ni(cod)$_2$][35] were prepared according to literature procedures.

***N*-Imidazolyl-4(24),6(10),12(16),18(22)-tetramethylenedioxy-2,8,14,20-tetrapentyl-resorcin[4]arene (5):** A mixture of tetrabromocavitand **4** (1.268 g, 1.12 mmol), imidazole (0.091 g, 1.34 mmol), K_2CO_3 (0.385 g, 2.79 mmol), DMEDA (0.074 g, 0.84 mmol) and CuI (0.160 g, 0.84 mmol) was dissolved in DMF (20 mL) and the reaction mixture was stirred at 140 °C for one week. After cooling to room temperature, water (50 mL) and $CHCl_3$ (50 mL) were added to the mixture. The organic layer was separated and the aqueous phase was extracted with $CHCl_3$ (2 × 50 mL). The combined organic layers were washed with aqueous 0.2 M Na_4EDTA (3 × 50 mL), the organic layer was dried with Na_2SO_4, and the solvent was removed under reduced pressure. The crude product was purified by flash chromatography (MeOH/CH_2Cl_2, 1:99, *v*/*v*) to afford a mixture (0.309 g; M1) of di- and tribrominated mono-imidazolyl-cavitands (R_f in the range 0.64–0.55 MeOH/CH_2Cl_2, 4:96, *v*/*v*), and a minor mixture (M2) of resorcinarenes substituted by two or more imidazolyl groups. *n*-Butyllithium (1.6 M in hexane, 1.37 mmol) was slowly added to a solution of M1 (0.309 g) in THF (10 mL) at –78 °C. After 0.5 h, the reaction was quenched with methanol (0.5 mL) and water (10 mL). The organic phase was recovered and the aqueous phase was washed with CH_2Cl_2 (2 × 10 mL) and the combined organic phases were dried with Na_2SO_4. After filtration, the solution was evaporated to dryness to afford **5** (0.290 g, overall yield 30%). The NMR spectra of the product were identical to those reported previously for **5**.[32]

General Procedure for Nickel-Catalysed Kumada–Tamao–Corriu Cross-Coupling Reactions: A 10 mL-Schlenk tube was filled with a solution of [Ni(cod)$_2$] in dioxane, a solution of the ligand in dioxane, aryl halide (0.5 mmol), PhMgBr (1 M in THF, 1 mL, 1.0 mmol), and decane (0.05 mL, internal reference). Dioxane was then added so that the total reaction volume was either 1.5 or 0.75 mL, and the reaction mixture was heated for 1 h at 100 °C. After cooling to room temperature, a small amount (0.5 mL) of the resulting solution was passed through a Millipore filter and analyzed by GC. All products were unambiguously identified by NMR spectroscopic analysis after their isolation. The NMR spectra were compared to those reported in the literature. Some homocoupling product (Ph-Ph) was detected in each run, but the Ph-Ph/Ar-Ph ratio never exceeded 15% (see the Supporting Information).

Crystallography: Single crystals of **1**·2*i*Pr_2O suitable for diffraction study were obtained by slow diffusion of diisopropyl ether into a dichloromethane solution of the imidazolium salt. M_r = 2420.88, triclinic, space group $P\bar{1}$, a = 16.0120(5), b = 19.6770(5), c = 24.2760(8) Å, α = 110.758(3), β = 98.915(3), γ = 105.457(2)°, V = 6624.1(3) Å^3, Z = 2, D_x = 1.214 mg m^{-3}, λ(Mo-K_α) = 0.71073 Å, μ = 0.678 mm^{-1}, F(000) = 2600, T = 120(2) K. Data were collected with an Oxford Diffraction Xcalibur Saphir 3 diffractometer (graphite Mo-K_α radiation, λ = 0.71073 Å). The structure was solved with SIR-97,[36] which revealed the non-hydrogen atoms of the molecule. After anisotropic refinement, many hydrogen atoms were located through Fourier difference analysis. The whole structure was refined with SHELX-97[37] and full-matrix least-square techniques (use of F^2; x, y, z, b_{ij} for C, Br, N and O atoms, x, y, z in riding mode for H atoms); 1495 variables and 15133 observations with $I > 2.0\sigma(I)$; calcd. $w = 1/[\sigma^2(F_o^2) + (0.1462P)^2 + 13.4589P]$ where $P = (F_o^2 + 2F_c^2)/3$. $R1$ = 0.0752, $wR2$ = 0.2657, S_w = 0.862, $\Delta\rho < 1.188$ e Å^{-3}. Crystallographic data for this structure have been deposited with the Cambridge Crystallographic Data Centre under deposition number CCDC-814000. These data can be obtained free of charge from The Cambridge Crystallographic Data Centre via www.ccdc.cam. ac.uk/data_request/cif.

Single crystals of **2**·*i*Pr_2O·1.25CH_2Cl_2 suitable for diffraction study were obtained by slow diffusion of diisopropyl ether into a dichloromethane solution of the imidazolium salt. M_r = 2428.85, triclinic, space group $P\bar{1}$, a = 16.0333(7), b = 19.3429(8), c = 24.567(1) Å, α = 73.138(4), β = 73.940(4), γ = 74.245(4)°, V = 6853.6(5) Å^3, Z = 2, D_x = 1.177 mg m^{-3}, λ(Mo-K_α) = 0.71073 Å, μ = 0.749 mm^{-1}, F(000) = 2578, T = 120(2) K. Data were collected on an Oxford Diffraction Xcalibur Saphir 3 diffractometer (graphite Mo-K_α radiation, λ = 0.71073 Å). The structure was solved with SIR-97,[36] which revealed the non-hydrogen atoms of the molecule. After anisotropic refinement, many hydrogen atoms were located through a Fourier difference analysis. The whole structure was refined with SHELX-97[37] and full-matrix least-square techniques (use of F^2; x, y, z, b_{ij} for C, Br, Cl, N and O atoms, x, y, z in riding mode for H atoms); 1400 variables and 8973 observations with $I > 2.0\sigma(I)$; calcd. $w = 1/[\sigma^2(F_o^2) + (0.11P)^2]$ where $P = (F_o^2 + 2F_c^2)/3$. $R1$ = 0.1067, $wR2$ = 0.3061, S_w = 0.888, $\Delta\rho < 1.898$ e Å^{-3}. The alerts level A in the cif file are mainly due to the large thermal motions of the C39···C43 chain, of one of the *i*Pr_2O molecules and of the partial CH_2Cl_2 molecule. Crystallographic data for this structure have been deposited with the Cambridge Crystallographic Data Centre under deposition number CCDC-814023. This data can be obtained free of charge from The Cambridge Crystallographic Data Centre via www.ccdc.cam. ac.uk/data_request/cif.

Supporting Information (see footnote on the first page of this article): Synthesis and full characterisation of the imidazolium salts used in this study together with the corresponding ^1H and ^{13}C NMR spectra; general procedure and catalytic results for nickel-catalysed KTC cross-coupling experiments.

Acknowledgments

The authors thank the Scientific and Technological Research of Turkey (TÜBİTAK-BİDEB), International Research Fellowship Programme for a grant to N. S., and the French Agence Nationale de la Recherche (ANR) (ANR-12-BS07-0001-01-RESICAT) for financial support.

---

[1] R. J. P. Corriu, J. P. Masse, *J. Chem. Soc., Chem. Commun.* **1972**, 144–144.
[2] K. Tamao, K. Sumitani, M. Kumada, *J. Am. Chem. Soc.* **1972**, *94*, 4374–4376.
[3] M. Kumada, *Pure Appl. Chem.* **1980**, *52*, 669–679.
[4] K. Tamao, *J. Organomet. Chem.* **2002**, *653*, 23–26.
[5] *Metal-Catalyzed Cross-Coupling Reactions* (Eds.: A. de Meijere, F. Diederich), Wiley-VCH, Weinheim, Germany, **2004**.
[6] W. A. Herrmann, in: *Homogeneous Catalysis with Organometallic Compounds* (Eds.: B. Cornils, W. A. Herrmann), 2nd ed., Wiley-VCH, Weinheim, Germany, **2002**, p. 91.
[7] J.-P. Corbet, G. Mignani, *Chem. Rev.* **2006**, *106*, 2651–2710.
[8] C. Barnard, *Platinum Met. Rev.* **2008**, *52*, 38–45.
[9] P. W. N. M. van Leeuwen, P. C. J. Kamer, J. N. H. Reek, P. Dierkes, *Chem. Rev.* **2000**, *100*, 2741–2769.
[10] J.-C. Hierso, R. Smaliy, R. Amardeil, P. Meunier, *Chem. Soc. Rev.* **2007**, *36*, 1754–1769.
[11] D. Sémeril, M. Lejeune, C. Jeunesse, D. Matt, *J. Mol. Catal. A* **2005**, *239*, 257–262.
[12] L. Monnereau, D. Sémeril, D. Matt, L. Toupet, A. J. Mota, *Adv. Synth. Catal.* **2009**, *351*, 1383–1389.

[13] M. Itagaki, G. Suzukamo, K. Nomura, *Bull. Chem. Soc. Jpn.* **1998**, *71*, 79–82.
[14] L. Monnereau, D. Sémeril, D. Matt, *Chem. Commun.* **2011**, *47*, 6626–6628.
[15] L. Monnereau, D. Sémeril, D. Matt, *Adv. Synth. Catal*. **2013**, *355*, 1351–1360.
[16] L. Ackermann, R. Born, J. H. Spatz, D. Meyer, *Angew. Chem.* **2005**, *117*, 7382; *Angew. Chem. Int. Ed.* **2005**, *44*, 7216–7219.
[17] N. Şahin, H. El Moll, D. Sémeril, D. Matt, I. Özdemir, C. Kaya, L. Toupet, *Polyhedron* **2011**, *30*, 2051–2054.
[18] V. P. W. Böhm, T. Weskamp, C. W. K. Gstöttmayr, *Angew. Chem.* **2000**, *112*, 1672; *Angew. Chem. Int. Ed.* **2000**, *39*, 1602–1604.
[19] V. P. W. Böhm, C. W. K. Gstöttmayr, T. Weskamp, W. A. Herrmann, *Angew. Chem.* **2001**, *113*, 3500; *Angew. Chem. Int. Ed.* **2001**, *40*, 3387–3389.
[20] D. Kremzow, G. Seidel, C. W. Lehmann, A. Fürstner, *Chem. Eur. J.* **2005**, *11*, 1833–1853.
[21] S. F. Schneider, C. F. Rentzsch, A. Krüger, H. G. Raubenheimer, W. A. Herrmann, *J. Mol. Catal. A* **2007**, *265*, 50–58.
[22] Z. Xi, B. Liu, W. Chen, *J. Org. Chem.* **2008**, *73*, 3954–3957.
[23] F. Li, J. Jin Hu, L. Lin Koha, T. S. A. Hor, *Dalton Trans.* **2010**, *39*, 5231–5241.
[24] R. Jothibasu, K.-W. Huang, H. V. Huynh, *Organometallics* **2010**, *29*, 746–3752.
[25] K. Zhang, M. Conda-Sheridan, S. R. Cooke, J. Louie, *Organometallics* **2011**, *30*, 2546–2552.
[26] C. Chen, H. Qiu, W. Chen, *J. Organomet. Chem.* **2012**, *696*, 4166–4172.
[27] M. J. Iglesias, A. Prieto, M. C. Nicasio, *Org. Lett.* **2012**, *14*, 4318–4321.
[28] H. El Moll, D. Sémeril, D. Matt, M.-T. Youinou, L. Toupet, *Org. Biomol. Chem.* **2009**, *7*, 495–501.
[29] H. El Moll, D. Sémeril, D. Matt, L. Toupet, *Eur. J. Org. Chem.* **2010**, 1158–1168.
[30] H. El Moll, D. Sémeril, D. Matt, L. Toupet, *Adv. Synth. Catal.* **2010**, *352*, 901–908.
[31] H. El Moll, D. Sémeril, D. Matt, L. Toupet, J.-J. Harrowfield, *Org. Biomol. Chem.* **2012**, *10*, 372–382.
[32] N. Şahin, D. Sémeril, E. Brenner, D. Matt, I. Özdemir, C. Kaya, L. Toupet, *Chem. Cat. Chem.* **2013**, *5*, 1116–1125.
[33] E. Brenner, D. Matt, M. Henrion, M. Teci, L. Toupet, *Dalton Trans.* **2011**, *40*, 9889–9898.
[34] N. Yoshikai, H. Matsuda, E. Nakamura, *J. Am. Chem. Soc.* **2008**, *130*, 15258–15259.
[35] T. M. Gomes Carneiro, J. Dupont, M. Luke, D. Matt, *Quim. Nova* **1988**, *11*, 215–217.
[36] A. Altomare, M. C. Burla, M. Camalli, G. Cascarano, C. Giacovazzo, A. Guagliardi, A. G. G. Moliterni, G. Polidori, R. Spagna, *J. Appl. Crystallogr.* **1998**, *31*, 74–77.
[37] G. M. Sheldrick, *SHELXL-97, Program for the Refinement of Crystal Stuctures*, University of Göttingen, Germany, **1997**.

Received: March 7, 2013